PIMA-CT: Physical Model-Aware Cyclic Simulation and Denoising for Ultra-low-dose CT Restoration

Peng Liu 1 , Linsong Xu 2 , Garrett Fullerton 1 , Yao Xiao 1,3 , James-Bond Nguyen 1 , Zhongyu Li 2 , Izabella Barreto 4 , Catherine Olguin 4 , and Ruogu Fang 1,5,6,*

- ¹J. Crayton Pruitt Family Department of Biomedical Engineering, University of Florida, Gainesville, FL, USA
- ²School of Software Engineering, Xi'an Jiaotong University, Xi'an, China
- ³Department of Radiation Physics, University of Texas MD Anderson Cancer Center, Houston, TX, USA
- ⁴Department of Radiology, University of Florida, Gainesville, FL, USA
- ⁵Center for Cognitive Aging and Memory, McKnight Brain Institute, University of Florida, Gainesville, FL, USA
- ⁶Department of Electrical and Computer Engineering, Herbert Wertheim College of Engineering, University of Florida, Gainesville, FL, USA

Correspondence*: Ruogu Fang ruogu.fang@bme.ufl.edu

ABSTRACT

- 3 A body of studies has proposed to obtain high-quality images from low-dose and noisy Computed
- 4 Tomography (CT) scans for radiation reduction. However, these studies are designed for
- 5 population-level data without considering the variation in CT devices and individuals, limiting the
- 6 current approaches' performance, especially for ultra-low-dose CT imaging. Here, we incorporate
- 7 a physical anthropomorphic phantom model PIMA-CT with an unsupervised learning framework,
- 8 using a novel deep learning technique Cyclic Simulation and Denoising (CSD), to address the
- 9 limitations. We first acquired low-dose and standard-dose paired phantom CT scans and then
- initiations. We first acquired low dose and standard dose paired phantom of seans and then
- 10 developed two generative neural networks: noise simulator and denoiser. The simulator extracts
- real low-dose noise and tissue features from two separate image spaces (e.g., low-dose phantom
- model scans and standard-dose patient scans) into a unified feature space. Meanwhile, the
- denoiser provides feedback to the simulator on the quality of the generated noise. In this way, the
- 14 simulator and denoiser cyclically interact to optimize network learning and ease the denoiser to
- 15 simultaneously remove noise and restore tissue features. We thoroughly evaluate our method
- 16 for removing both real low-dose and Gaussian simulated low-dose noise. The results show that
- 17 CSD outperforms one of the state-of-the-art denoising algorithms without using any labeled data
- 18 (actual patients' low-dose CT scans) nor simulated low-dose CT scans. This study may shed light
- on incorporating physical models in medical imaging, especially for ultra-low level dose CT scan
- 20 restoration.
- 21 Keywords: Physical model, Medical image denoising, Low-dose CT, Noise removal, Dose reduction

1 INTRODUCTION

- 22 The quality of medical imaging is critical for diagnosis and treatments. However, medical imaging
- 23 often suffers from noise produced at either the image reconstruction or post-imaging stages. Medical
- 24 physicists in radiology play several essential roles in maintaining imaging quality and stability for imaging
- 25 machines, such as Computed tomography (CT). They usually adopt an anthropomorphic physical model
- 26 to facilitate the assessment of imaging quality and the adjustment of the imaging machines' parameters
- 27 before performing on real patients. Motivated by this, we hypothesized that a physical model could also
- 28 help restore high-quality images for the cases in the post-imaging stage, such as radiation reduction in CT
- 29 imaging.
- 30 Reducing radiation dose during imaging is a low-cost approach to release concerns about causing cancer or
- 31 other negative health conditions using CT scanning (1), but this method introduces noise into CT scans,
- 32 hindering the diagnostic effectiveness of such scans. Several studies (2, 3) have been proposed to address
- 33 this problem by removing the noise from low-dose CT scanned images. However, these studies are designed
- 34 based on Gaussian noise simulation for populations without considering the variation in CT devices and
- 35 individuals, limiting the current approaches' performance, especially for ultra-low-dose CT imaging (see
- 36 Figure 1A).
- 37 Moreover, most of the success of deep learning-based approaches for low-dose CT image restoration (4, 5)
- 38 much relies on a large number of labeled images. However, obtaining the real low-dose CT scans is not
- 39 available in practice. Accessing real image noise is critical for the development of any practical imaging
- 40 algorithm. Also, real noise properties significantly vary among different CT machines and individuals.
- 41 Thus, the Gaussian noise assumption is not always guaranteed in practical scenarios and significantly limits
- 42 the existing approaches for ultra-low-dose CT imaging.
- 43 We address these problems by incorporating an anthropomorphic physical phantom model into generative
- 44 adversarial networks. The proposed framework is named Cyclic Simulation and Denoising (CSD). The
- 45 physical model provides paired low-dose and standard-dose phantom CT scans before scanning the actual
- 46 patients. These phantom scans can offer statistical noise prior, which is related to the specific CT machine
- 47 for patient diagnosis, for CSD to precisely capture noise properties and remove real complex noise from
- 48 CT scans. Our CSD is composed of noise simulation and denoising two networks. The simulation network
- 49 facilitates the denoising network to learn real noise properties. The denoising network thus can access
- 50 realistic noise through physical phantom CT scans. However, phantom scans lack tissue features (see
- 51 Figure 1B). The missing tissue information prevents feasible phantom-based solutions for CT image
- 52 restoration. As one can see in Figure 1C, the model trained with paired low-dose and standard-dose
- 53 phantom scans fails to remove real noise from low-dose patient scans. To overcome this problem, we
- 54 train CSD using normal-dose and phantom CT scans simultaneously to embrace realistic noise and tissue
- of train CDD using normal dose and phantom CT seams sinultaneously to emorate realistic noise and tissue
- 55 features into a unified learning framework without the access labeled or Gaussian noise simulated data.
- 56 We evaluate our CSD for removing both real low-dose and Gaussian simulated noise. The results show
- 57 that CSD outperforms one of the state-of-the-art denoising algorithms for ultra low-quality medical image
- 58 restoration. Our main contributions include that (1) we incorporate an anthropomorphic physical phantom
- 59 model into generative adversarial learning to address the challenges of removing real noise from ultra-low-
- 60 dose CT scans for radiation reduction; (2) we develop a unsupervised framework in the combination of
- 61 phantom CT scans that can outperform one of the start-of-the-art methods without using any labeled or
- 62 other noise simulation data; (3) to the best of our knowledge, this is the first study to incorporate physical
- 63 model into deep learning for medical imaging.

2 MATERIALS AND METHODS

- 64 The problem of CT image denoising can be understood by L = H + N, where H is the clean, standard-
- dose CT image, L is the noisy, low-dose CT image, and N is additive image noise. Though an additive
- 66 relationship does not completely represent the relationship between clean and noisy images, this formula
- 67 provides a baseline for understanding the problem.
- 68 We utilize two deep networks in the framework. The first network G_s is the noise simulator and can be
- 69 modeled by $L = G_s(H, \alpha)$, where α is the desired simulated dose level and implicitly indicated in training
- 70 data. The second network G_d is the denoiser that can be modeled by $H = G_d(L)$, where G_d is the network
- 71 generating a clean image from a given low-dose noisy input L.

72 2.1 Unsupervised Learning by Incorporating Physical Model

- 73 We use a head phantom model to obtain paired low-dose and standard-dose phantom CT scans, with which
- 74 we combine the normal dose (standard-dose) patient CT scans to develop our CSD model. The phantom
- 75 scans allow the model to access real noise properties and the patient scans offer the actual brain tissue
- 76 features to the model. In this way, we eliminate the need for noisy low-dose CT scans from actual patients
- and even the Gaussian noise simulated low-dose CT scans to develop our mode (Figure 2A). Therefore,
- 78 we present an unsupervised learning framework by incorporating an anthropomorphic physical phantom
- 79 model.

80 2.2 Cyclic Simulation and Denoising (CSD)

81 2.2.1 Overview

- 82 We develop two deep networks to perform simulator and denoiser individually. To ease the network
- 83 training, we first use paired low-dose and standard-dose phantom CT scans to pre-train the simulator
- 84 and denoiser, separately. Then, we plug the simulator and denoiser pre-trained models into our CSD
- 85 framework (Figure 2A). In particular, we start with noise simulation using both the phantom and patient CT
- 86 scans to generate low-dose noisy patient CT images that simultaneously provide noise and tissue features
- 87 for training the denoiser (Figure 2B). Meanwhile, CSD also allows the backward training process from
- 88 denoiser to simulator. The denoiser takes phantom noisy scans and simulated noisy patient scans as input to
- 89 learn how to remove realistic noise and restore tissue features simultaneously, while the simulator mainly
- 90 plays as a regularizer to the denoiser for stabilizing the training (Figure 2B). The interaction between
- 91 simulator and denoiser forms a dynamic data-driven framework, named Cyclic Simulation and Denoising
- 92 (CSD), to address the challenges of low-dose CT image restoration.

93 2.2.2 Pretrain Simulator and Denoiser $(H o \widehat{L}, L o \widehat{H})$

- 94 We train the simulator with a u-shape encoder-decoder generative adversarial network by formulating the
- objective as an adverarial learning. We use a discriminator D_s to differentiate real low-dose CT images
- from fake samples generated by the simulator G_s . We illustrate the formulation of the simulation as below.

$$\mathcal{L}_{GAN}(G_s, D_s) = \mathbb{E}_{L \sim p(L)}[\log(\mathbf{D}_s(L))] + \mathbb{E}_{H_{phantom} \sim p(H)}[\log(1 - \mathbf{D}_s(\mathbf{G}_s(H_{phantom})))]$$
(1)

To encourage the output of the denoiser to match the clean phantom scans, we use an ℓ_1 loss between the output and the ground truth image.

$$\mathcal{L}_1(G_d) = \mathbb{E}_{L, H \sim p(L, H)} \| H - \mathbf{G}_d(L) \|_1 \tag{2}$$

- 99 Initializing the weights by pretraining can significantly ease the convergence of two interactive generators
- 100 in both spatial and temporal space. However, the phantom scans still lack the essential features as scanning
- 101 on a real patient.
- 102 2.2.3 Learn Simulation Interacting with Denoiser: S2D $(H o \widehat{L} o \widehat{H})$
- 103 We start with noise simulation to provide both noise and tissue features for training denoiser. We apply a
- 104 discriminator D_s to train the simulator G_s . We formulate the simulation objective as below.

$$\mathcal{L}_{GAN}^{S2D}(G_s, D_s) = \mathbb{E}_{L \sim p(L)}[\log(\mathbf{D}_s(L))] + \mathbb{E}_{H \sim p(H)}[\log(1 - \mathbf{D}_s(\mathbf{G}_s(H)))]$$
(3)

- 105 The simulator feeds its output into the denoiser during training. Thus, we formulate the denoising loss
- 106 using a modified Equation 2 as below.

$$\mathcal{L}_1^{S2D}(G_d) = \mathbb{E}_{L,H \sim p(L,H)} \left\| H - \mathbf{G}_d(\mathbf{G}_s(H)) \right\|_1 \tag{4}$$

- 107 Besides the discriminator D_s , we take advantage of the denoising performance as regularization feedback
- 108 to indicate the quality of the simulation. As the simulation becomes better, the denoising is getting harder.
- Furthermore, the simulator D_s in S2D takes the standard-dose scans from both phantom and patients as
- inputs. The phantom data apples a latent constrain to the D_s and stabilizes the training. Interacting with
- denoising encourages the simulator to generate realistic low-dose noise. Further, the denoise can benefit of
- taking the output of the simulator as additional training data, dynamically.
- 113 2.2.4 Learn Denoising in Simulator: D2S $(L o \widehat{H} o \widehat{L})$
- 114 The development of the training process from denoising to simulation has two significant varies from the
- 115 cycle consistency study (6) (see Figure 2(c)). We first enable supervised learning to train the denoiser G_d
- using the standard-dose and the corresponding low-dose CT images. Compared to the adversarial learning,
- 117 supervised learning provides a stronger supervision signal to build an accurate denoiser. More importantly,
- 118 the simulator in S2D produces the noise gradually close to the desired level during training. Thus, we can
- acquire various noise level images from the simulator, with which, the denoiser-self implicitly learns to
- 120 restore clean CT scans for a range level of low-dose CT scans, rather than a specific noise level indicated in
- 121 the training data. Therefore, the input to the denoiser G_d in D2S includes phantom low-dose and simulated
- 122 patient low-dose images. We use a ℓ_1 loss to train the denoiser G_d . The ℓ_1 loss encourages a pixel-wise
- 123 match to the ground-truth. We illustrate the ℓ_1 loss as below.

$$\mathcal{L}_{1}^{D2S}(G_{d}) = \mathbb{E}_{L, H \sim p(L, H)} \| H - \mathbf{G}_{d}(L) \|_{1}$$
(5)

- Besides, we use adversarial learning to train the simulator in D2S to match the desired noise distribution in
- the actual low-dose CT scans. The objective to this adversarial learning the distribution is written as below.

$$\mathcal{L}_{GAN}^{D2S}(G_s, D_s) = \mathbb{E}_{L \sim p(L)}[\log(\mathbf{D}_s(L))] + \mathbb{E}_{\hat{H} \sim p(H)}[\log(1 - \mathbf{D}_s(\mathbf{G}_s(\hat{H})))] \quad (6)$$

We develop the cyclic simulation and denoising training with regularizations in both directions and take advantage of both cycles $H \to \widehat{L} \to \widehat{H}$ and $L \to \widehat{H} \to \widehat{L}$. The total objective is illustrated as below.

$$G_{s}^{*}, G_{d}^{*} = \arg \min_{G_{s}, G_{d}} \max_{D_{s}} \lambda_{1} \mathcal{L}_{GAN}^{S2D}(G_{s}, D_{s}) + \lambda_{2} \mathcal{L}_{1}^{S2D}(G_{d}) + \lambda_{3} \mathcal{L}_{GAN}^{D2S}(G_{s}, D_{s}) + \lambda_{4} \mathcal{L}_{1}^{D2S}(G_{d})$$
(7)

- where λ indicates the weights of each loss. With these novel developments, the simulator and denoiser
- 129 interact each other in a cyclic self-learning manner to enable realistic noise simulation and accurate
- 130 denoising for low-dose CT image.

3 RESULTS

131 **3.1 Datasets**

- 132 We use three CT datasets during training and testing. The first dataset is obtained from the CT scanning
- on a single tissue-equivalent physical phantom model. This set contains various levels of low-dose series,
- scanned between 5 mAs and 95 mAs with 5 mAs intervals (see examples in the supplementary Figure S1).
- 135 In this work, we simply use 20 mAs, 30 mAs, and 60 mAs low-dose phantoms for training noise simulation
- and evaluating the reality of various types of noise in Figure 1C. We also include the standard-dose (175)
- mas) scans as the ground-truth. Each dose level of phantom series produces 138 CT scans. The second
- 138 dataset is a public Retrospective Image Registration Evaluation (RIRE) dataset. This dataset includes 388
- 139 standard-dose CT scans. We use 80% for training the simulator and denoiser in the proposed CSD and
- 140 also task 20% for demonstrating the advantages of CSD over end-to-end training a denoiser in Table 2,
- where we simulate the low-dose noise by adding Gaussian noise on normal dose CT scans. We compute
- the corresponding standard variation of Gaussian noise for a specific mAs by following (7). Additionally,
- 143 we acquire a real patient dataset including paired standard-dose (190 mAs) and low-dose (20 mAs) in a
- 144 total of 432 CT scans (see examples in the supplementary Figure S2). We use them for comparing various
- 145 types of simulated noise in Figure 1C and evaluating real noise removal performance of our approach in
- to type of simulated noise in Figure 12 and evaluating fear noise femous performance of our approach in
- 146 Table 1, where 250 scans are used for training and 182 scans are used for testing. Moreover, we randomly
- select 373 scans from this dataset combining with 20% of the RIRE dataset, in total 449 scans included, to
- 148 evaluate our CSD's generalizability in Table 2.

149 3.2 Evaluation Metric

- 150 We develop CSD with U-net (8) for the simulator network G_s and DnCNN (9) for the denoiser network G_d .
- 151 We evaluate image denosing performance using Peak signal-to-noise ratio (PSNR) and image structural
- 152 similarity index measure (SSIM).

153 3.3 Unsupervised Learning Performance on Real Low-dose Noise Removal

- 154 Here, we aim to demonstrate that the proposed CSD framework in a combination with phantom can remove
- 155 the real low-dose noise effectively. We first take the start-of-the-art medical image denoising network (9)
- as a baseline and train it with Gaussian simulated low-dose CT scans at different noise levels. Then, we
- build the G_d in CSD using the baseline's architecture and train it with paired low-dose and standard-dose
- 158 phantom CT scans at the same noise levels as Gaussian simulation. We test each model on 182 real low-dose
- 159 CT scans at the noise level 20 mAs. The comparison results are shown in Figure 1C at 20 mAs and Table 1
- 139 C1 scans at the horse level 20 mAs. The comparison results are shown in Figure 1C at 20 mAs and Table 1
- at 30, 60 mAs noise levels. As one can see, the combination of the proposed CSD training framework and
- phantom simulation significantly outperforms the baseline with an average 1.56 dB improvement on PSNR

across three different noise levels. Furthermore, as one can see in Figure 1C, the baseline network, which is trained with paired low-dose and standard-dose phantom scans, performs much worse than the model trained with both our CSD phantom and Gaussian simulation, which may be due to the lack of critical tissue features in the phantom scans. Notably, these results may indicate that *CSD*, in combination with phantom simulation, can encourage the denoiser to learn both real low-dose noise features from phantom and tissue image features from patient scans, simultaneously, and leading to real low-dose noise removal with greater accuracy and precision.

169 3.4 Evaluate CSD's generalizability (Ablation without G_s)

Here, we further evaluate the proposed CSD's generalizability to train a denoiser targeting the general 170 simulated low-dose noise, such as Gaussian simulation. We still use the same baseline network to conduct this study. We use the standard end-to-end manner and our CSD framework to train two networks with 172 the same architecture as the baseline, separately. Notably, to have a fair comparison, we only use original 173 noisy CT scans in training dataset as the input of the G_d in D2S cyclic training. Then, we compare the two networks to remove 30 and 60 mAs levels of Gaussian simulated low-dose noise from 449 CT scans. 175 As one can see in Table 2, the model trained with our CSD can consistently outperform the one trained 176 with end-to-end manner, with impressive average performance gain 0.355 dB for PSNR. In addition, we 177 also show a visual result comparison in Figure 3. As one can see, the denoiser G_d trained with our CSD 178 framework can produce more realistic CT scans from its low-dose noisy version. More visual results of 179 low-dose simulation and denoising can be found in the supplementary Figure S3 and Figure S4. These 180 results suggest that starting with simulation may create a live environment from which the denoiser can 181 learn high-validity representations to achieve a better denoising performance. Theoretically, the simulator 182 and denoiser in the CSD may play as a regularizer to each other to optimize the networks effectively. 183

4 CONCLUSION

This paper proposed incorporating an anthropomorphic physical phantom model with generative deep learning networks for medical imaging, with a focus on realistic low-dose CT image restoration. The 185 combination of an anthropomorphic physical model with deep generative adversarial networks can 186 eliminate the needs of both actual low-dose patients and even other low-dose simulation CT scans to 187 build an unsupervised learning framework for low-dose CT image restoration. More importantly, an 188 anthropomorphic physical model CT scanning can abstract the unique noise properties of a particular CT 189 imaging machine for the deep learning model to take CT machine domain variation into account during 190 training. Eventually, with the interaction between a noise simulation network and a denoising network 191 192 in cyclic training processing, the proposed deep learning model embraces realistic noise from low-dose phantom CT scans and tissue features from normal-dose patient CT scan into a single unified framework 193 194 for building a state-of-the-art method for real low-dose CT image restoration.

CONFLICT OF INTEREST STATEMENT

195 The authors declare that the research was conducted in the absence of any commercial or financial relationships that could be construed as a potential conflict of interest.

AUTHOR CONTRIBUTIONS

- 197 PL, YX, and RF contributed to conception and design of the study. PL, GF, YX, and JN organized the
- 198 database. PL, LX, and ZL contributed to the software used in this study. PL performed the statistical
- 199 analysis. IB and CO provided digital scanning data of the anthropomorphic physical phantom. PL and
- 200 GF wrote the first draft of the manuscript. PL, GF, YX, and RF wrote sections of the manuscript. RF was
- 201 responsible for supervision, project administration, and funding acquisition. All authors contributed to
- 202 manuscript revision, read, and approved the submitted version.

FUNDING

This material is based upon work supported by the National Science Foundation under Grant No. (NSF 1908299).

SUPPLEMENTARY MATERIAL

205 Supplementary Material is available for this paper.

DATA AVAILABILITY STATEMENT

- 206 Publicly available datasets were analyzed in this study. This data can be found here: https://rire.insight-
- 207 journal.org/download_training_data.html. Anonymized data are available from the corresponding authors
- 208 upon reasonable request. The code and software used in this study will be made publicly available upon
- 209 acceptance.

REFERENCES

- 1 .Goldman A, Maldijian P. Reducing radiation dose in body CT: A practical approach to optimizing CT
 protocols. *American Journal of Roentgenology* 200 (2013) 748–754.
- 212 2 .Badretale S, Shaker F, Babyn P, Alirezaie J. Fully convolutional architecture for low-dose CT image
- 213 noise reduction. IOP Conference Series: Materials Science and Engineering (Hawaii, USA: International
- 214 Conference on Artificial Intelligence Applications and Technologies) (2017), vol. 261, 012012.
- 215 3. Yang Q, Yan P, Zhang Y, Yu H, Shi Y, Mou X, et al. Low-dose CT image denoising using a generative
- adversarial network with wasserstein distance and perceptual loss. IEEE transactions on medical
- 217 *imaging* **37** (2018) 1348–1357.
- 4 . Yang Q, Yan P, Kalra MK, Wang G. CT image denoising with perceptive deep neural networks. *ArXiv* abs/1702.07019 (2017).
- 5. Chen H, Zhang Y, Zhang W, Liao P, Li K, Zhou J, et al. Low-dose CT denoising with convolutional
- neural network. 2017 IEEE 14th International Symposium on Biomedical Imaging (ISBI 2017) (IEEE)
- 222 (2017), 143–146.
- 6. Zhu JY, Park T, Isola P, Efros AA. Unpaired image-to-image translation using cycle-consistent adversarial
- networks. *Proceedings of the IEEE international conference on computer vision* (2017), 2223–2232.
- 7 .Britten A, Crotty M, Kiremidjian H, Grundy A, Adam E. The addition of computer simulated noise to investigate radiation dose and image quality in images with spatial correlation of statistical noise: an
- example application to X-ray CT of the brain. *The British journal of radiology* **77** (2004) 323–328.

8 .Ronneberger O, Fischer P, Brox T. U-net: Convolutional networks for biomedical image segmentation.
 Navab N, Hornegger J, Wells WM, Frangi AF, editors, *International Conference on Medical Image Computing and Computer-Assisted Intervention (MICCAI)* (Cham: Springer) (2015), 234–241.

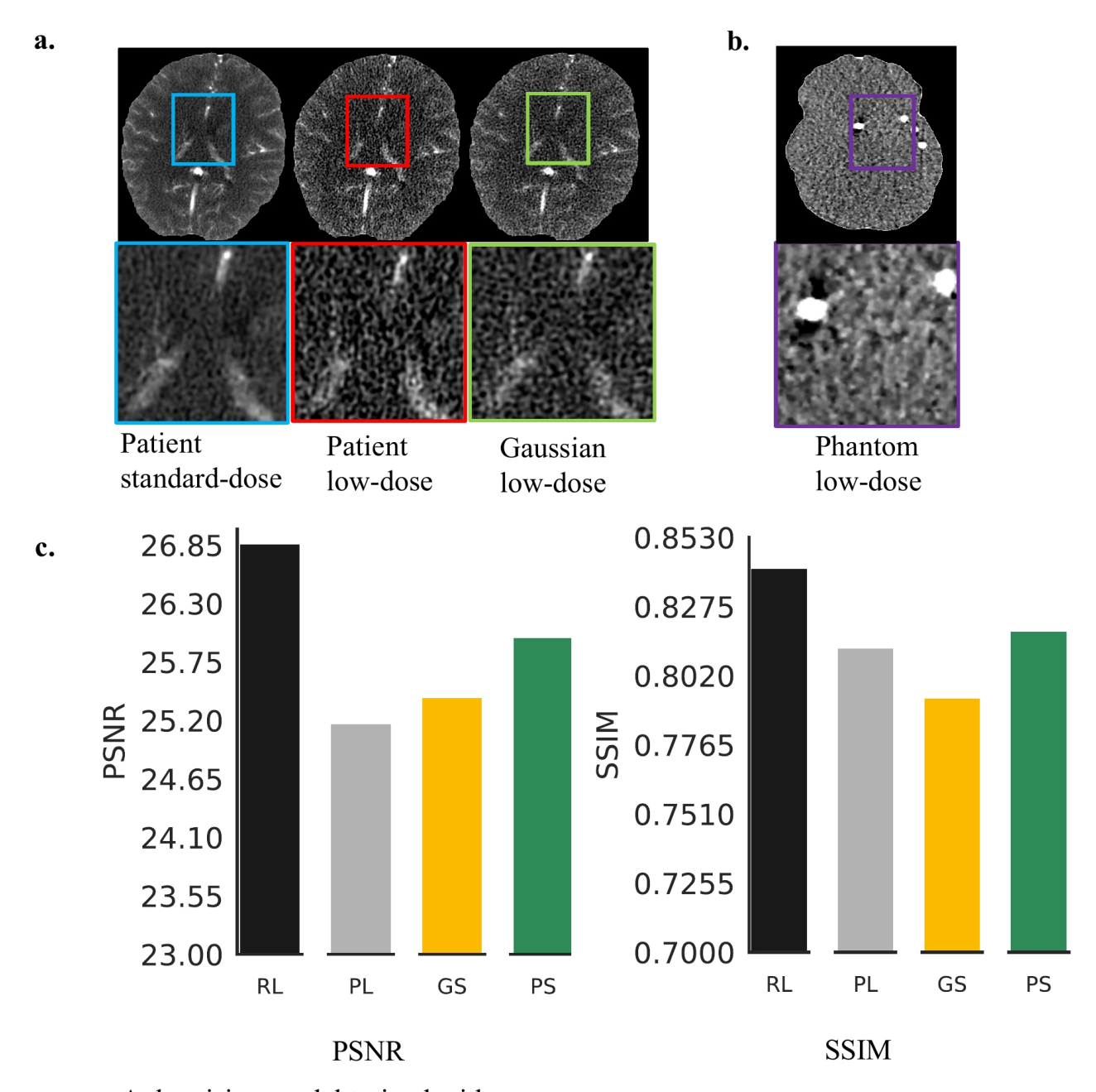
9 .Zhang K, Zuo W, Chen Y, Meng D, Zhang L. Beyond a gaussian denoiser: Residual learning of deep cnn for image denoising. *IEEE Transactions on Image Processing* **26** (2017) 3142–3155.

Table 1. The average real low-dose noise removal performance of a same deep neural network *trained* with Gaussian noise simulation and CSD + physical phantom noise simulation, separately. The best results are highlighted in bold.

PSNR (dB) / SSIM			
Noise level (mAs) Trained with Gaussian Trained with CSD + phantom			
30 60	24.47/0.7555 23.03/0.6960	26.10/0.8235 25.51/0.7894	

Table 2. The average Gaussian noise removal performance of the same deep neural network trained through the proposed CSD framework and the standard end-to-end manner, separately. The best results are highlighted in bold.

PSNR (dB) / SSIM Noise level (mAs) End-to-end training CSD training			
30	31.93/0.9105	32.05/0.9124	
60	33.33/0.9365	33.92/0.9429	



A denoising model trained with:

RL: real low- and standard-dose paired patient CT scans

PL: real low- and standard-dose paired phantom CT scans

GS: Gaussian simulated low- and standard-dose paired CT scans

PS: our CSD incorporating with physical phantom model

Figure 1. Real low-dose has a different noise distribution from Gaussian noise and is hard to remove. (**A**) It shows a visual comparison of the standard-dose CT, real low-dose CT, and Gaussian simulated low-dose CT scans. (**B**) It shows a low-dose CT scanned by using a physical phantom model. (**C**) We trained four same structural deep neural networks(DNNs) using various types of low-dose noise with the same noise level (20 mAs radiation dose) and then compared the effectiveness of noise removal.

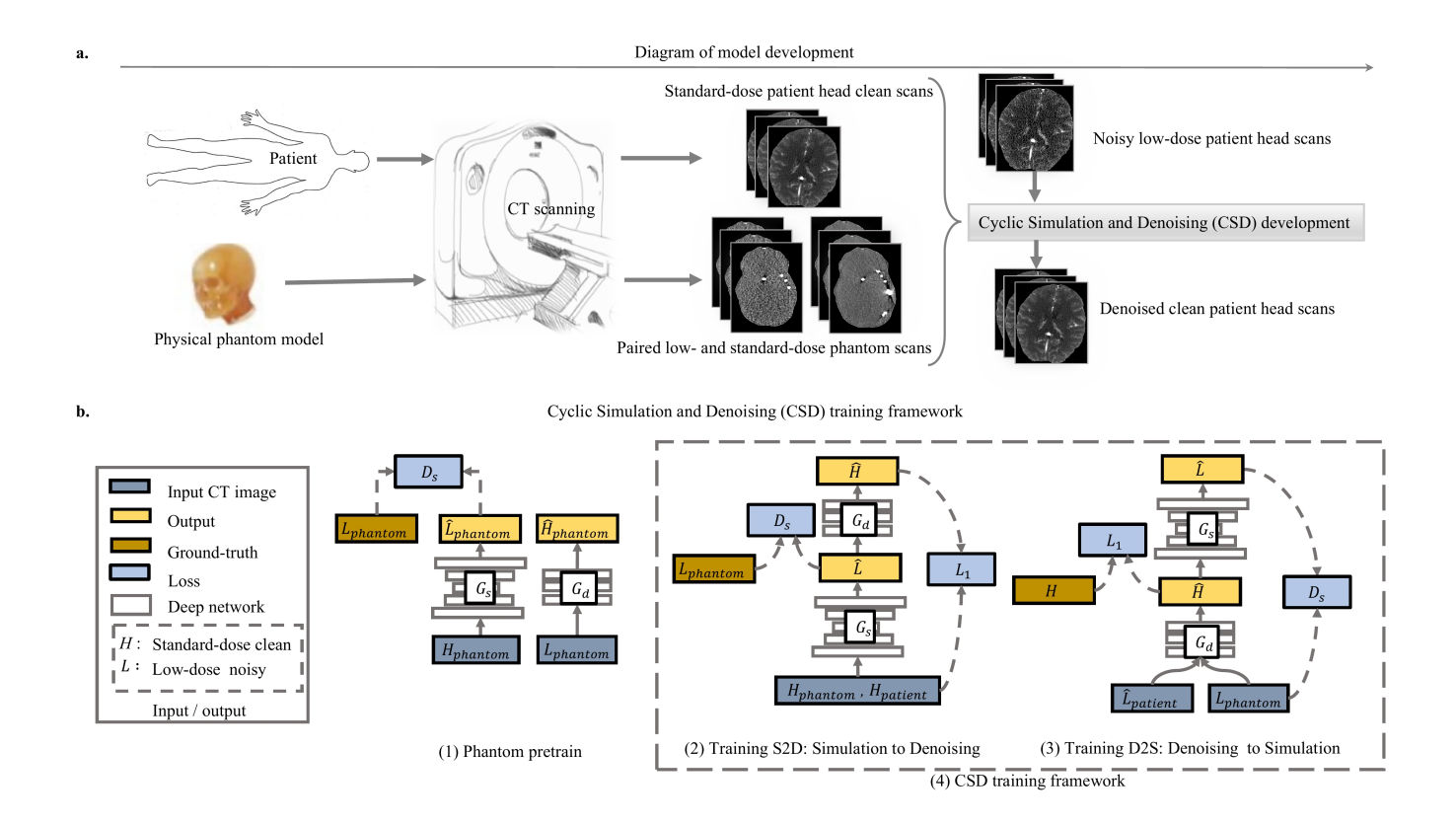


Figure 2. The overview of the model development in (**A**) and the proposed CSD training framework in (**B**). (**A**) demonstrates how we incorporate a physical phantom model into the proposed deep learning model CSD. (**B**) shows how our CSD is developed in detailed. Two training stages: first, we initialize the weights of simulator and denoiser by pretrain on physical phantom CT scan (1); second, the cycle-training from noise simulation to denoising (2) and another cycle-training from denoising to simulation (3) are developed, simultaneously. The G_s and G_d represent simulation and denoising, separately. During training, the two cycles interact with each other and are executed, alternatively.

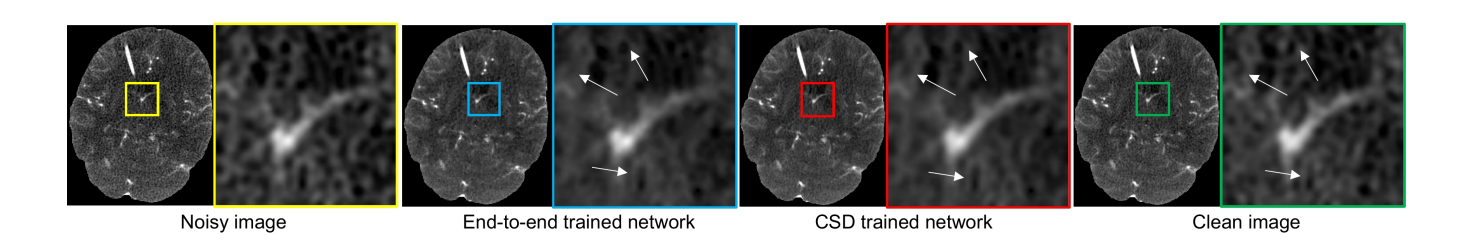


Figure 3. The visual comparison of the denoising performance between the network trained with end-to-end and the one trained with our CSD framework.